Macromolecules
ARTICLE

Macromolecules **2009**, *42*, 6483–6494 **6483**
DOI: 10.1021/ma901248m

Synthesis of Complementary Host- and Guest-Functionalized Polymeric Building Blocks and Their Self-Assembling Behavior

Minjae Lee,[†] Daniel V. Schoonover,[†] Anthony P. Gies,[‡] David M. Hercules,[‡] and Harry W. Gibson*,[†]

[†]*Department of Chemistry, Virginia Polytechnic & State University, Blacksburg, Virginia 24061, and* [‡]*Department of Chemistry, Vanderbilt University, Nashville, Tennessee 37235*

Received June 10, 2009; Revised Manuscript Received July 30, 2009

ABSTRACT: New polymers that incorporate paraquat or crown ether moieties as chain ends or central units were synthesized by stable free radical polymerization (SFRP) and atom transfer radical polymerization (ATRP). For SFRP, TEMPO derivatives that contain a functional unit were used as initiators. For ATRP, a copper−amine or copper−bipyridine complex was used as a catalyst with radical initiators from halide derivatives of paraquat and crown ethers. These end- or center-functionalized polymers formed pseudorotaxane complexes with complementary small molecules. They also formed reversible pseudorotaxane polymers: chain-extended, star-shaped homopolymers, and block copolymers. Complexation studies to determine stoichiometry and association constants with thermodynamic parameters were performed by NMR spectroscopy and isothermal microcalorimetric (ITC) titration. The association constants of crown ether derivatives and paraquat compounds in chloroform were measured for the first time: $K_a = 2.97 \times 10^3\ M^{-1}$ for paraquat polystyrene and bis(*m*-phenylene)-32-crown-10 and $K_a = 4.38 \times 10^3\ M^{-1}$ for paraquat polystyrene and crown ether polystyrene. These are 4−6-fold higher than the association constant of the analogous small molecule host−guest system in acetone.

Introduction

Since the synthesis and characterization of 18-crown-6 in 1967,[1] many crown ethers have been synthesized, and their complexation behaviors have been widely studied.[2] Crown ethers can undergo complexation not only with metal ions but also with rodlike cationic molecules to form threaded structures known as pseudorotaxanes and rotaxanes.[3] The convergence of supramolecular and polymer science has also led to the construction of analogues of traditional macromolecules by supramolecular methods. Because of their unique topological character and potential functions, these systems may lead to advancements in many applications.[4] Some previous examples of polymers formed by the self-assembly of the host and guest units include dendrimers from cooperative complexation of a homotritopic guest and complementary monotopic dendron hosts,[5] a hyperbranched polymer from an AB_2 monomer,[6] linear polymers from self-organization of well-defined building blocks,[7] a supramolecular triarm star polymer from a homotritopic host and a complementary monotopic paraquat-terminated polystyrene guest,[8] and polymers with terminal pseudorotaxane units from polymers end-functionalized with crown ethers and small guest molecules.[9]

The formation of pseudorotaxanes from crown ethers and *N*, *N*′-dialkyl-4,4′-bipyridinium salts ("paraquats") was confirmed by X-ray crystallography, and their association constants (K_a) were determined by various analytical tools. The K_a of bis(*m*-phenylene)-32-crown-10 (BMP32C10) and dimethylparaquat bis(hexafluorophosphate) was reported as 760 M^{-1} in acetone-d_6 at ambient temperature.[4a] The association constants between host and guest molecules can be changed through the variation of system parameters, such as temperature, pH, solvent, and impurities. In the phenylene crown ether complexes with paraquats, the main intermolecular forces for complexations are multiple hydrogen bonds, dipole−dipole, and π-electron interactions between the host and guest. Since the complexations occur in solution, solvent effects are important. For example, protic solvents (such as methanol) interfere with the hydrogen bonding between the host and guest. Polar aprotic solvents (such as DMSO and DMF) can also lower the binding forces due to their high polarity and hydrogen bond accepting character. For this reason, higher association constants are expected in less polar solvents; however, the paraquat compounds are almost insoluble even in THF and other less polar solvents. The association constants between crown ethers and paraquat species have been measured in acetone or acetonitrile (MeCN) due to the need for a common solvent for the host and guest molecules. We expected that the association constants of crown ethers and paraquat derivatives could be higher in solvents less polar than acetone or MeCN; however, no one has reported the association values in less polar solvents due to the poor solubilities of the paraquat compounds.

Herein, we first report pseudorotaxane formation in chloroform from paraquat-functionalized polystyrene and crown ethers (**1** in Figure 1) and from center-functionalized polystyrene and paraquat (**2** in Figure 1). From polymeric building blocks that contain a terminal crown ether or paraquat unit, chain extension (**3**) and 3-armed star polymers (**4**) were observed in solution (Figure 1). Diblock copolymer and 3-armed star copolymer formation from polystyrenes and PMMA with functional complementary host−guest terminal units were also tried (**5**, **6**); however, they were less efficient than the polystyrene homopolymer systems. The details are discussed below.

Experimental Section

Isothermal Microcalorimetric (ITC) Titrations. Samples of the host and guest molecules were accurately weighed into volumetric flasks and diluted to volume with solvent to yield stock solutions for titration. Titrations were run on a Microcal MCS

*Corresponding author: e-mail hwgibson@vt.edu; Fax 540-231-8517; Tel 540-231-5902.

Published on Web 08/11/2009

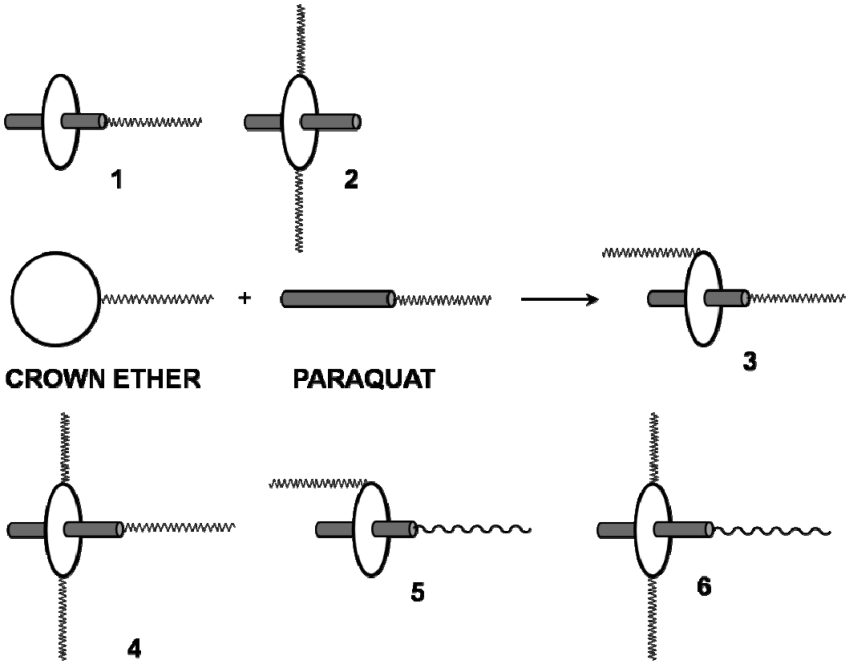

Figure 1. Cartoon representations of the formation of polymers with a terminal (**1**) or central pseudorotaxane unit (**2**), chain extension by pseudorotaxane formation from host- and guest-terminated polymers (**3**), 3-armed star polymers by pseudorotaxane formation (**4**), block copolymers by pseudorotaxane formation (**5**), and 3-armed block copolymers by pseudorotaxane formation (**6**).

ITC. Raw isotherm data were collected using the Microcal Observer software. Integration and fitting of the isothermal data (K_a and ΔH) were accomplished using Origin software with a one set of sites algorithm. The titration curve was fit using the Weisman isotherm, yielding ΔH. The Gibbs free energy was calculated from the association constant, K_a: $\Delta G = -RT \ln K_a$. Then ΔS was calculated from $\Delta S = (\Delta H - \Delta G)/T$.

MALDI-TOF/TOF CID Measurements. All samples were analyzed using a Voyager Elite DE STR MALDI-TOF MS (Applied Biosystems, Framingham, MA) equipped with a 337 nm N_2 laser. All spectra were obtained in the positive ion mode using an accelerating voltage of 20 kV and a laser intensity of ~10% greater than threshold. The grid voltage, guide wire voltage, and delay time were optimized for each spectrum to achieve the best signal-to-noise ratio. All spectra were acquired in the reflectron mode with a mass resolution greater than 3000 fwhm; isotopic resolution was observed throughout the entire mass range detected. External mass calibration was performed using protein standards from a Sequazyme Peptide Mass Standard Kit (Applied Biosystems) and a five-point calibration method using Angiotensin I (m = 1296.69 Da), ACTH (clip 1−17) (m = 2093.09 Da), ACTH (clip 18−39) (m = 2465.20 Da), ACTH (clip 7−38) (m = 3657.93 Da), and bovine insulin (m = 5730.61 Da). Internal mass calibration was subsequently performed using a PEG standard (M_n = 2000; Polymer Source, Inc.) to yield monoisotopic masses exhibiting a mass accuracy better than $\Delta m = \pm 0.1$ Da. The instrument was calibrated before every measurement to ensure constant experimental conditions. All samples were run in a dithranol or 3-aminoquinoline (3AQ) matrix doped with silver trifluoroacetate (AgTFA), copper(II) chloride ($CuCl_2$), or with no cationization agent added ("neat"). Samples were prepared using the dried-droplet method with weight (mg) ratios of 50:10:1 (dithranol:polymer:AgTFA) in THF. After vortexing the mixture for 30 s, 1 μL of the mixture was pipetted on the MALDI sample plate and allowed to air-dry at room temperature. MS data were processed using the Data Explorer 4.9 software supplied by the manufacturer (Applied Biosystems).

Materials. The preparations of the paraquat and crown ether precursors for SFRP (TEMPO derivatives) and ATRP initiators followed literature procedures.[10,11] Styrene (Aldrich) and methyl methacrylate (Aldrich) were filtered through basic alumina and stored under nitrogen. The monomers and dimethylformamide (DMF) were deoxygenated by nitrogen bubbling for at least 30 min before polymerization. Copper(I) bromide (Aldrich) was washed with glacial acetic acid, vacuum-filtered, washed with absolute ethanol, and dried in a vacuum oven. 2,2′-Dipyridyl was recrystallized from ethanol and dried in a vacuum oven. Acetonitrile (MeCN) for esterification reactions of acid chlorides and alcohols was distilled over calcium hydride. Pyridine was distilled over sodium hydroxide and stored under nitrogen. All other chemicals and solvents were used as received.

***N*-(*ω*-Carboxypentyl)-4,4′-bipyridinium PF_6^- (7).** A solution of 4,4′-dipyridyl (9.38 g, 60 mmol) and 6-bromohexanoic acid (1.95 g, 10 mmol) in MeCN (30 mL) was refluxed for 2 days. The precipitate was filtered after cooling and then washed with MeCN three times. The bromide salt was dissolved in deionized water (30 mL), and KPF_6 (2.76 g, 15 mmol) was added. The precipitate was filtered and washed with deionized water twice. Drying in a vacuum oven gave an off-white crystalline solid **7** (3.45 g, 83% yield); mp 143.3−144.6 °C (dec). ^{1}H NMR (400 MHz, DMSO-d_6, 23 °C): δ 1.33 (m, 2H), 1.56 (m, 2H), 1.97 (m, 2H), 2.24 (t, J = 7, 2H), 4.63 (t, J = 7, 2H), 8.05 (d, J = 7, 4H), 8.64 (d, J = 7, 2H), 8.89 (s, 2H), 9.23 (d, J = 7, 2H), 12.07 (br, 1H). ^{13}C NMR (100 MHz, DMSO-d_6, 23 °C): δ 23.8, 24.9, 30.4, 33.3, 60.3, 122.0, 125.4, 140.9, 145.3, 151.0, 152.3, 174.4. HR ESI MS: m/z 271.1454 ([M − PF_6^-]$^+$, calcd for [M − PF_6^-]$^+$ 271.1441, error 2.9 ppm).

***N*-(*ω*-Carboxypentyl)-*N*′-methyl-4,4′-bipyridinium $2PF_6^-$ (8).** Into a solution of **7** (1.380 g, 2.50 mmol) in dry MeCN (10 mL), iodomethane (0.780 g, 5.5 mmol) was added at room temperature. The mixture was refluxed for 3 days. After removing volatile materials, water (20 mL) and KPF_6 (0.55 g, 28 mmol) were added. The mixture was stirred at 60 °C for 3 h, and the precipitate was filtered, recrystallized from water twice, and dried in a vacuum oven. A yellow crystalline solid, 1.100 g (76%), mp 181.1−183.3 °C (dec), was obtained. ^{1}H NMR (400 MHz, acetone-d_6, 23 °C): δ 1.53 (m, 2H), 1.68 (m, 2H), 2.24 (m, 2H), 2.32 (m, 2H), 4.74 (s, 3H), 4.99 (t, J = 8, 2H), 8.84 (m, 4H), 9.37 (d, J = 7, 2H), 9.47 (d, J = 7, 2H). ^{13}C NMR (100 MHz, acetone-d_6, 23 °C): δ 24.8, 26.1, 31.9, 33.7, 49.4, 62.9,

127.7, 128.1, 146.9, 147.8, 150.6, 150.9, 174.5. HR ESI MS: m/z 431.1306 ($[M - PF_6^-]^+$, calcd for $[M - PF_6^-]^+$ 431.1318, error 2.8 ppm).

***N*-Methyl-*N*′-{ω-[(2-phenyl-2-(2′,2′,6′,6′-tetramethylpiperidine-*N*-oxyl)ethoxycarbonyl]pentyl}-4,4′-bipyridinium $2PF_6^-$ (10).** A mixture of **8** (0.5966 g, 1.035 mmol) and freshly distilled thionyl chloride (6 mL) was stirred at 50 °C for 12 h under a nitrogen atmosphere. After removing the excess $SOCl_2$ by vacuum distillation, the residue was rinsed with anhydrous ethyl ether five times. The corresponding carbonyl chloride of **8** was a dark-yellow solid; its identity was confirmed by ^{1}H NMR. Into a solution of the carbonyl chloride in dry MeCN (15 mL), **9** (0.2871 g, 1.035 mmol) was added, and then dry pyridine (0.0860 g, 1.09 mmoL) was added dropwise over 10 min in an ice bath. After stirring for 3 days at room temperature, the insoluble materials were filtered, and the solvent was removed from the filtrate by rotoevaporation. The residue was dissolved in ethyl acetate (EA) (80 mL), and the solution was washed with water three times. The organic solution was dried over anhydrous Na_2SO_4, and the drying agent was filtered. After removing the EA by a rotoevaporator, the residual solid was washed with ethyl ether three times and dried in a vacuum oven at 50 °C: 0.823 g (95%) of beige (off-white) solid; mp 182.2−186.5 °C (dec). ^{1}H NMR (400 MHz, acetone-d_6, 23 °C): δ 0.69 (s (br), 3H), 1.05−1.65 (m, 19H), 2.10−2.27 (m, 4H), 4.28 (m, 1H), 4.61 (m, 1H), 4.92 (t, J = 8, 2H), 4.97 (s (br), 1H), 7.29−7.40 (m, 5H), 8.80 (m, 4H), 9.37 (d, J = 7, 2H), 9.47 (d, J = 7, 2H). ^{13}C NMR (100 MHz, acetone-d_6, 23 °C): δ 17.7, 20.6, 24.7, 26.1, 31.8, 34.1, 41.1, 49.4, 60.7, 62.8, 66.3, 84.9, 127.7, 128.1, 128.7, 128.9, 146.8, 147.8, 150.6, 150.9, 173.1. HR ESI MS: m/z 836.2978 ($[M + H]^+$, calcd for $[M + H]^+$ 836.2974, error 0.5 ppm), m/z 690.3257 ($[M - PF_6]^+$, calcd for $[M - PF_6^-]^+$ 690.3254, error 0.5 ppm).

SFRP of Styrene To Form 11 (Bulk Polymerization), Target DP = 300. A mixture of **1** (0.1298 g, 0.155 mmol) and styrene monomer (4.843 g, 46.5 mmol) was stirred at 125 °C for 15 h. After 15 h, the magnetic stir bar was stopped by the high viscosity. The mixture was cooled to room temperature and dissolved in chloroform (20 mL). The solution was added slowly to MeOH (450 mL) with vigorous stirring. The precipitated solid was filtered and dissolved again in 20 mL of chloroform. The solution was added to 450 mL of MeOH with vigorous stirring. The precipitated solid was dissolved in THF (15 mL) and precipitated into MeOH (450 mL). Filtration and drying in a vacuum oven gave 3.440 g (69%) of fine colorless powder. SEC: M_n = 31.5 kDa, PDI = 1.19 (THF, light scattering detector, PS standards calibration). ^{1}H NMR (400 MHz, $CDCl_3$, 22 °C): δ 1.5−2.3 (m, br), 3.96 (m, br), 4.18 (s, 3H, br), 4.38 (br), 6.6−7.3 (m, br), 8.20 (d, 4H, br), 8.67 (s, 4H, br).

SFRP of Styrene To Form 11 (Solution Polymerization), Target DP = 300. A mixture of **10** (0.2925 g, 0.350 mmol) and styrene monomer (10.936 g, 105 mmol) in DMF (5 mL) was stirred at 125 °C for 8 h. The mixture was cooled to room temperature and dissolved in chloroform (30 mL). The solution was added slowly to 750 mL of MeOH with vigorous stirring. The precipitated solid was filtered and then dissolved in chloroform (30 mL). The solution was added to MeOH (750 mL) with vigorous stirring. The precipitated solid was dissolved in THF (20 mL) and precipitated into MeOH (750 mL). Filtration and drying in a vacuum oven gave 9.665 g (86%) of light pink fine powder. SEC: M_n = 31.5 kDa, PDI = 1.07 (THF, light scattering detector, PS standards calibration). ^{1}H NMR (400 MHz, $CDCl_3$, 22 °C): δ 1.5−2.3 (m, br), 3.97 (br), 4.17 (s, 3H, br), 4.38 (br), 6.6−7.3 (m, br), 8.21 (d, 4H, br), 8.69 (s, 4H, br).

***N*-[2-(α-Bromoisobutyryloxy)ethyl]-*N*′-methyl-4,4′-bipyridinium $2PF_6^-$ (12).** Into a solution of *N*-(2-hydroxyethyl)-*N*′-methyl-4,4′-bipyridinium PF_6^-[13] (2.531 g, 5.00 mmol) and pyridine (0.475 g, 6.00 mmol) in dry MeCN (15 mL) in an ice bath, α-bromoisobutyryl bromide (1.150 g, 5.00 mmol) was added by a syringe over 10 min. After stirring for 15 h at room temperature, the insoluble materials were removed by filtration, and the solution was concentrated. The residue was dispersed in water (60 mL), and the insoluble product was filtered. After washing the filter cake three times with water, drying in a vacuum oven at 50 °C gave 2.57 g (76%) of beige (off-white) crystalline solid; mp 181.9−183.7 °C (dec). ^{1}H NMR (400 MHz, DMSO-d_6, 23 °C): δ 1.85 (s, 6H), 4.43 (s, 3H), 4.72 (t, J = 4, 2H), 5.08 (t, J = 4, 2H), 8.75 (d, J = 7, 2H), 8.85 (d, J = 7, 2H), 9.28 (d, J = 7, 2H), 9.42 (d, J = 7, 2H). ^{13}C NMR (100 MHz, DMSO-d_6, 23 °C): δ 30.4, 48.5, 57.2, 59.8, 64.4, 110.0, 126.5, 126.8, 146.9, 147.1, 148.3, 149.6, 170.7. HR ESI MS: m/z 509.0427 ($[M - PF_6^-]^+$, calcd for $[M - PF_6^-]^+$ 509.0423, error 0.8 ppm).

ATRP of MMA To Form 13, Target DP = 100. A mixture of **12** (0.1640 g, 0.250 mmol), CuBr (0.0360 g, 0.250 mmol), 2,2′-dipyridyl (0.1172 g, 0.75 mmol), and methyl methacrylate (2.503 g, 25.0 mmol) in DMF (2.5 g) was stirred at 90 °C for 12 h. The mixture was cooled to room temperature and dissolved in THF (15 mL). The copper catalyst was removed through a Celite pad. The filtrate was concentrated to 3 mL and then added slowly to MeOH (60 mL) with vigorous stirring. The precipitated solid was filtered and then dissolved in chloroform (10 mL). The solution was filtered through a Celite pad a second time to remove the green, precipitated copper catalyst. The filtrate was added slowly to MeOH (60 mL) with vigorous stirring. Filtration and drying in a vacuum oven gave 1.10 g (41%) of pale yellow powder. SEC: M_n = 40.7 kDa, PDI = 1.33 ($CHCl_3$, RI detector, PS standards calibration). ^{1}H NMR (400 MHz, $CDCl_3$, 22 °C): δ 0.8−1.0 (s + s, br), 1.2 (s, br), 1.4 (m, br), 1.8−2.1 (m, br), 3.6 (s), 4.7 (m, 3H), 8.7−8.9 (m, 4H), 9.2−9.5 (m, 4H).

5-Chloroacetoxymethyl-1,3-phenylene-*p*-phenylene-33-crown-10 (14). Into a solution of monohydroxymethyl-MPPP33C10[14] (0.710 g, 1.26 mmol) and chloroacetyl chloride (0.180 g, 1.51 mmol) in dry chloroform (10 mL), triethylamine (0.152 g, 1.5 mmol) was slowly added over 10 min in an ice bath. After the reaction mixture was stirred for 3 days at room temperature, water (15 mL) was added, and the mixture was extracted with chloroform (20 mL) three times. The combined organic layer was washed with saturated aqueous $NaHCO_3$ and then water. The solution was dried over Na_2SO_4, and the drying agent was removed by filtration. After the solvent was removed by a rotoevaporator, flash column chromatography (EA/silica gel) gave a colorless, viscous oil 0.490 g (60%). ^{1}H NMR (400 MHz, $CDCl_3$, 22 °C): δ 3.69 (m, 16H), 3.82 (m, 8H), 4.02 (m, 8H), 4.11 (s, 2H), 5.11 (s, 2H), 6.40 (s, 1H), 6.50 (s, 2H), 6.78 (s, 4H). ^{13}C NMR (100 MHz, $CDCl_3$, 22 °C): δ 39.9, 66.6, 66.7, 67.2, 68.6, 68.7, 69.8, 69.9, 100.3, 106.0, 114.7, 135.9, 152.0, 159.1, 170.1. HR FAB MS (NBA-PEG): m/z 642.2405 (calcd for M^+ 642.2443, error 5.9 ppm).

ATRP of Polystyrene To Form 15, Target DP = 300. A mixture of **14** (0.129 g, 0.20 mmol), CuBr (0.0861 g, 0.60 mmol), 2,2′-dipyridyl (0.281 g, 1.80 mmol), and styrene (6.25 g, 60 mmol) in phenyl ether (6 g) was stirred at 130 °C for 8 h. The mixture was cooled to room temperature and then dissolved in chloroform (15 mL). The catalyst was removed by passage through a short basic alumina column. The eluent was concentrated to 10 mL volume and then slowly added to MeOH (250 mL) with vigorous stirring. The precipitated solid was filtered and dissolved in 10 mL of chloroform. The chloroform solution was slowly added to MeOH (250 mL) with vigorous stirring. Filtration and drying in a vacuum oven gave 1.40 g (22%) of white powder. SEC: M_n = 21.4 kDa, PDI = 1.29 ($CHCl_3$, RI detector, PS standards calibration). ^{1}H NMR (400 MHz, $CDCl_3$, 22 °C): δ 1.2−2.3 (m, br), 3.67 (s, 16H), 3.79 (m, 8H), 4.01 (m, 8H), 6.3−7.4 (m, br).

Bis(5-chloroacetoxymethyl-1,3-phenylene)-32-crown-10 (16). Into a solution of bis(5-hydroxymethyl-1,3-phenylene)-32-crown-10[14] (0.579 g, 1.00 mmol) and chloroacetyl chloride (0.163 mL, 2.10 mmol) in chloroform (10 mL) in an ice bath, pyridine (0.163 mL, 2.10 mmol) was added by syringe over 30 min. After the mixture had stirred for 3 days at room temperature, saturated $NaHCO_3$ solution (15 mL) was added, and the product was extracted with chloroform (20 mL) three

Scheme 1. Synthesis of Paraquat-Terminated Polystyrene 11 by SFRP

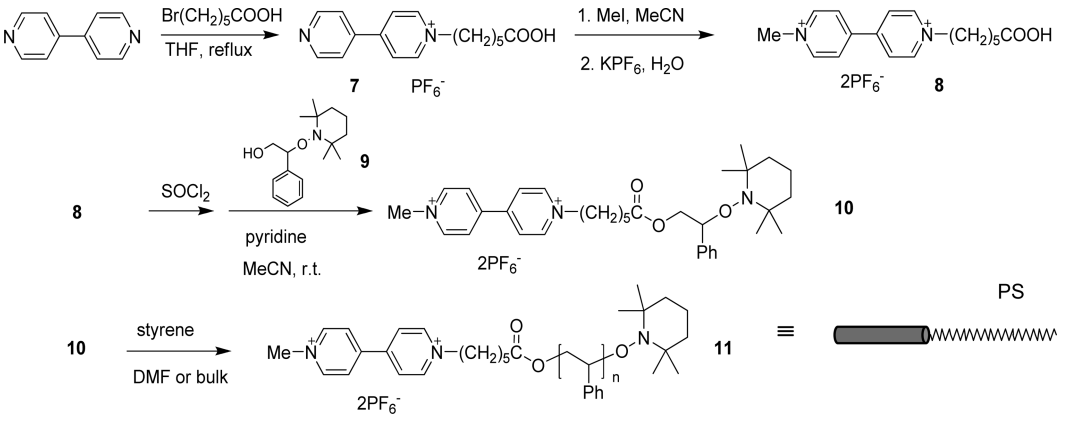

times. The combined organic layer was washed with 1 M HCl solution, saturated aqueous $NaHCO_3$, and then water. The solution was dried over anhydrous Na_2SO_4, and the drying agent was removed by filtration. The solvent was removed by a rotoevaporator to give a colorless oil, 0.694 g (92%). The oil solidified after 1 day at room temperature; mp 90.1−91.8 °C. ^{1}H NMR ($CDCl_3$, 22 °C): δ 3.70 (m, 17H (theor 16H)), 3.83 (t, J = 4.6 Hz, 8H), 4.05 (t, J = 4.6 Hz, 8H), 4.08 (s, 4H), 5.10 (s, 4H), 6.43 (t, J = 2.2 Hz, 2H), 6.49 (d, J = 2.2 Hz, 4H). ^{13}C NMR ($CDCl_3$, 22 °C): δ 40.9, 67.6, 67.7, 69.6, 70.9, 101.5, 107.0, 136.9, 160.1, 167.1. HR FAB MS (NBA-PEG): m/z 748.2199 (calcd for M^+ 748.2265, error 4.5 ppm).

ATRP of Styrene To Form 17, Target DP = 100. A mixture of **16** (0.209 g, 0.28 mmol), CuBr (0.160 g, 1.16 mmol), 2,2′-dipyridyl (0.545 g, 3.48 mmol), and styrene (2.91 g, 28.0 mmol) in phenyl ether (3 g) was stirred at 130 °C for 8 h. The mixture was cooled to room temperature and dissolved in chloroform (15 mL). The catalyst was removed by passage through a short basic alumina column. The eluent was concentrated to 3 mL and then added slowly to MeOH (50 mL) with vigorous stirring. The precipitated solid was filtered and dissolved in 5 mL of chloroform. The chloroform solution was added slowly to MeOH (50 mL) with vigorous stirring. Filtration and drying in a vacuum oven gave 2.30 g (74%) of white powder. SEC: M_n = 13.5 kDa, PDI = 1.25 ($CHCl_3$, light scattering detector, PS standards calibration). ^{1}H NMR (400 MHz, $CDCl_3$, 22 °C): δ 1.2−2.3 (m, br), 3.67 (s, 16H), 3.80 (m, 8H), 4.01 (m, 8H), 6.3−7.4 (m, br).

Results and Discussion

Preparation of Polymeric Building Blocks. Paraquat-terminated polymers were synthesized by controlled radical polymerization (CRP). For stable free radical polymerization (SFRP), a paraquat−TEMPO initiator **10** was synthesized (Scheme 1). In the preparation of **7** an excess of 4,4′-bipyridine was used to prevent the formation of the disubstituted bipyridinium side product. Paraquat carboxylic acid **8** was prepared by methylation of the resulting monosubstituted compound **7**. The paraquat−TEMPO initiator **10** was formed by the esterification of **8** and 2-phenyl-2-(2′,2′,6′,6′-tetramethylpiperidine-*N*-oxyl)ethanol (**9**).

Polystyrenes with terminal paraquat units (**11**) were synthesized with the paraquat−TEMPO initiator **10** in solution or in bulk. The reaction temperature was maintained at 120−130 °C for 8−13 h. DMF was used as a solvent for the solution polymerization because it dissolves both polystyrene and the polar paraquat initiator **10**. The viscosity of the reaction mixture increased as the polymerization proceeded. In the bulk process the reactions were terminated when the magnetic stirrer stopped. In the first stage of the bulk polymerization, the initiator **10** was not completely soluble in styrene monomer. However, when the polymerization was complete, the initiator was completely consumed, and there was no insoluble solid. Therefore, these SFRP reactions of styrene allowed good control of the molecular weight (from the ratio of the monomer and the initiator) and relatively narrow polydispersities (below 1.20) by both methods. The ^{1}H NMR spectrum of **11** in $CDCl_3$ clearly shows the paraquat protons at δ 8.2 and 8.7. The number-average molecular weights calculated from integration of the NMR spectra correspond to the size exclusion chromatography (SEC) results well (THF, PS standards) (Table 1).

Table 1. Molecular Weights Estimated by ^{1}H NMR Spectroscopy and SEC for the Paraquat-Terminated Polystyrenes (11) by SFRP

polymerization method	target M_n (kDa)	M_n (NMR) (kDa)	M_n (SEC) (kDa)	PDI (SEC)
SFRP, bulk	31.2	33.7	31.5	1.19
SFRP, solution	31.2	37.5	31.5	1.07

A paraquat-terminated poly(methyl methacrylate) (PMMA) was synthesized by ATRP. The paraquat ATRP initiator **12** was prepared by esterification of *N*-methyl-*N*′-(β-hydroxyethyl)-4,4′-bipyridinium bis(hexafluorophosphate) with α-bromoisobutyryl bromide. The ATRP of methyl methacrylate (MMA) with the initiator **12** was performed using copper(I)/2,2′-bipyridyl as catalyst in DMF at 90 °C (Scheme 2). The ^{1}H NMR spectrum of **13** in $CDCl_3$ clearly shows the paraquat protons at δ 8.8 and 9.3. The chemical shifts of the paraquat protons are different between **11** and **13**, even though the terminal paraquat structure is same (*N*-methylparaquat). The reason for the chemical shift changes must be due to the different polymer structures; hydrocarbon polystyrene and oxygen-rich PMMA. The PMMA chain induces a deshielding effect on the paraquat protons. The more polar polymer provides a local environment that is similar to acetone-d_6, in which dimethyl paraquat's aromatic protons appear at 8.8 and 9.4 ppm.[15a] This may be ascribed to interaction (some would say hydrogen bonding) of the aromatic paraquat protons with the oxygen atom of acetone solvent or the PMMA ether and carbonyl oxygen atoms. The number-average molecular weight (M_n) was 40.7 kDa (targeted M_n 10.0 kDa), and the PDI was 1.33 from SEC analysis (THF, PS standards). The molecular weight of synthesized **13** was higher than target molecular weight due to the poor solubility of copper(I)/2,2′-dipyridyl catalyst in methyl methacrylate (monomer) during the polymerization.

A crown ether-terminated polystyrene was synthesized using the ATRP initiator **14** (Scheme 3). **14** was prepared by the esterification of 5-hydroxymethyl-1,3-phenylene-*p*-phenylene-33-crown-10 (MPPP33C10) with chloroacetyl

Scheme 2. Synthesis of Paraquat-Terminated PMMA 13 by ATRP

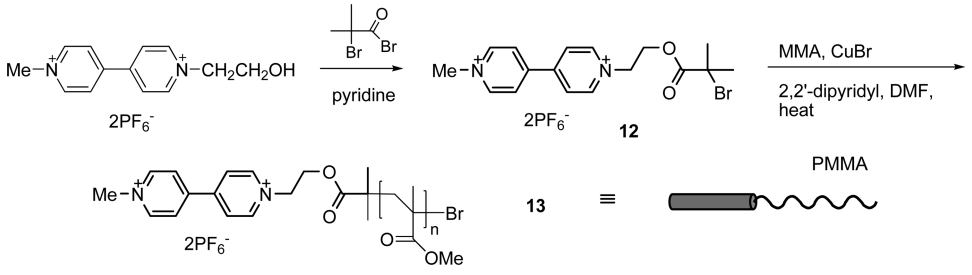

Scheme 3. Synthesis of Crown Ether (MPPP33C10)-Terminated Polystyrene 15 by ATRP

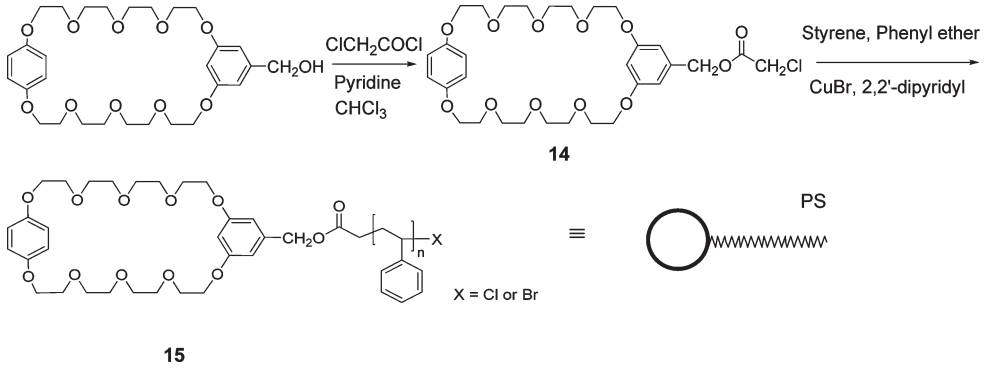

Scheme 4. Synthesis of Crown Ether (BMP32C10)-Centered Polystyrene 17 by ATRP

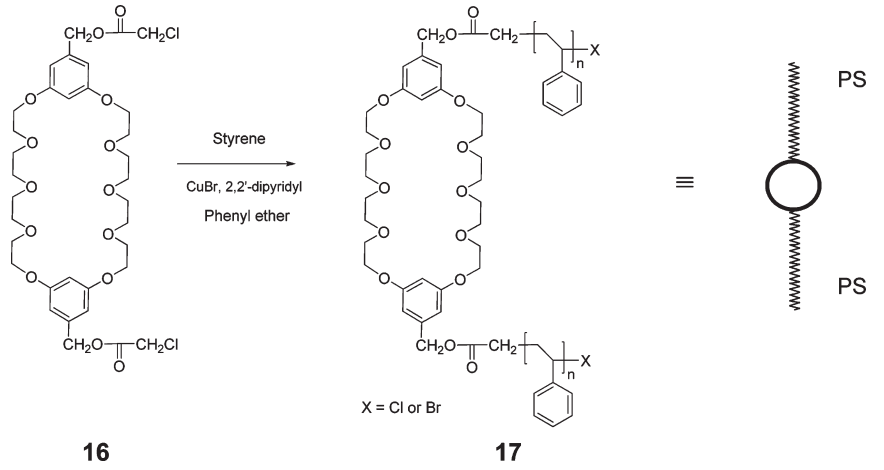

chloride. In the ATRP, 3 equiv of copper(I) bromide and 9 equiv of 2,2′-dipyridyl were used per initiator **14**. No polymerization occurred if only 1 or 2 equiv of catalyst was added; we hypothesize that radical generation from the copper(I)/2.2′-dipyridyl catalyst is prevented by crown ether complexation of up to 2 equiv of copper(I) ion. The number-average molecular weight (M_n) of this crown-terminated polystyrene **15** was 21.4 kDa (targeted M_n = 31.3 kDa), and the PDI was 1.29 from SEC analysis (THF, PS standards).

A crown ether-centered polystyrene was also prepared by ATRP (Scheme 4) from the dichlorobis(*m*-phenylene)-32-crown-10 (BMP32C10) ATRP initiator **16**. 4 equiv of copper(I) bromide and 12 equiv of 2,2′-dipyridyl per initiator **16** were used in the ATRP reaction. The number-average molecular weight (M_n) of the crown-centered polystyrene **17** was 13.5 kDa (targeted M_n = 10.4 kDa), and the PDI was 1.25 by SEC ($CHCl_3$, PS standards).

MALDI-TOF Mass Spectrometric Analysis of the Polymeric Building Blocks. MALDI-TOF mass spectrometric results for polystyrene **11** in 3-anthraquinoline are shown in Figure 2. The spectrum contains series of four peaks each. The sequential sets of peaks are separated by 104 mass units, corresponding to the styryl repeat unit. In the two main series of peaks after loss of a TEMPO moiety (156 Da) and hydrogen, presumably via *N*-hydroxytetramethylpiperidine, the paraquat end groups are clearly observed: (1) the polymer after loss of two PF_6 ions (**11**-2PF_6-TEMPO-H)$^+$, structure **18**, m/z 1010 (n = 7), 1114 (n = 8), and 1218 (n = 9), and (2) the polymer after loss of a benzylidene group (**11**-2PF_6-TEMPO-H-C_6H_5CH)$^+$, structure **19**: m/z 1024 (n = 7), 1128 (n = 8), 1232 (n = 9). The polymers with one PF_6 ion are also observed but as weaker peaks: (**11**-PF_6-TEMPO-H-C_6H_5CH)$^+$, structure **18** + PF_6, m/z 1040 (n = 6), 1144 (n = 7), 1248 (n = 8) and (**11**-PF_6-TEMPO-H)$^+$; structure **19** + PF_6, m/z 1054 (n = 6), 1159 (n = 7), 1263 (n = 8). The loss of TEMPO in MALDI-TOF mass analysis has been already reported by Vairon et al.[12] In agreement with the report of Gibson et al.,[9] structure **19** (=CH_2 end) predominates in this high mass range over structure **18** (benzylidene end, =CHC_6H_5). The loss of the benzylidene group is

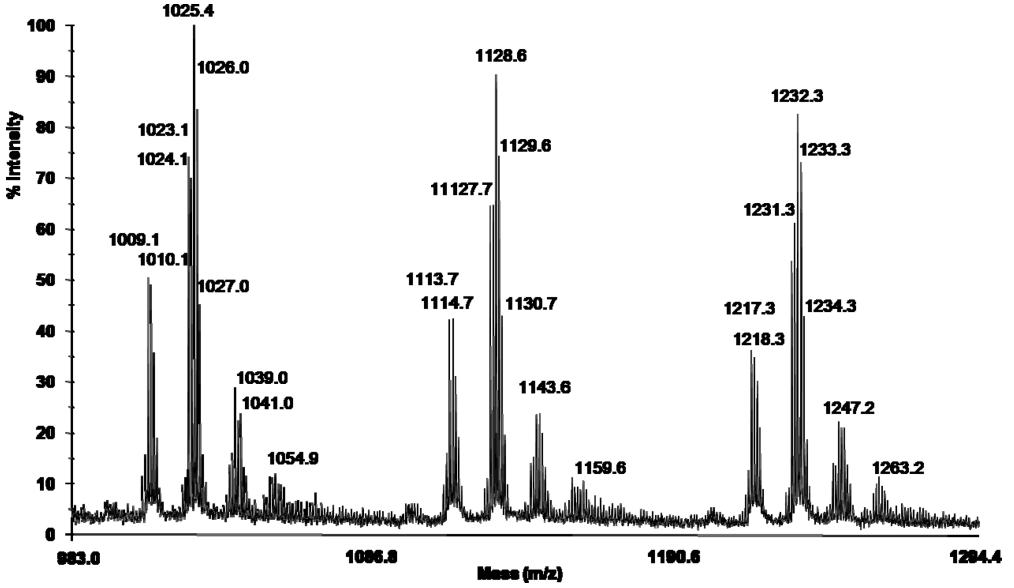

Figure 2. Partial MALDI-TOF mass spectrum (covering mass range 980−1295 Da) of paraquat-terminated polystyrene **11**. Sample prepared by the D-D method in 3AQ with no added cationization agent.

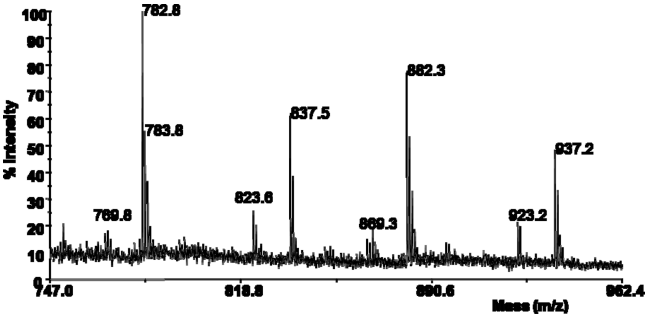

Figure 3. Partial MALDI-TOF mass spectrum (covering mass range 747−962 Da) of paraquat-terminated PMMA **13**. Sample prepared by the D-D method in 3AQ with no added cationization agent.

believed to occur via loss of *N*-benzyloxytetramethylpiperidine.

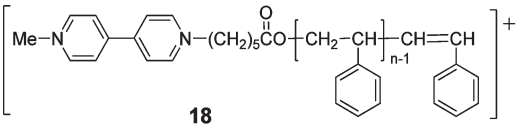

18

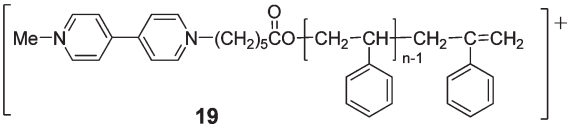

19

MALDI-TOF mass spectrometric results for paraquat-terminated poly(methyl methacrylate) sample **13** in 3-anthraquinoline are shown in Figure 3. The sequential pairs of peaks are separated by 100 mass units, corresponding to the methyl methacrylate repeat unit. The paraquat end group is clearly observed as with the paraquat-terminated polystyrene. No brominated species are observed. The series with the strongest signals correspond to structure **20** with loss of two PF_6 species (presumably one as the anion and the other as HPF_6, as often observed[14,15]): m/z 782 ($n = 5$) and 882 ($n = 6$). The next most prominent series of peaks are due to **21** formed by cleavage of the PMMA main chain by rearrangement: m/z 838 ($n = 5$) and 937 ($n = 6$). Rearrangements of PMMA during mass spectrometry were reported by Scrivens et al., and they proposed the mechanisms shown in Schemes 5 and 6.[13] Because no cationization agent was used for this sample, we believe that only the charges are associated with the paraquat moieties of **20** and **21**. The two ways to form structure **20**, the loss of HBr from the end of **13** and the cleavage of the backbone as in Scheme 5, are consistent with the higher peak intensities corresponding to structure **20** versus those corresponding to structure **21**, which can form only via the pathway shown in Scheme 6. The next strongest series of peaks is attributed to $[\mathbf{21} - CH_2]^+$: m/z 824 ($n = 5$) and 923 ($n = 6$). The weakest series of signals is assigned to $[\mathbf{20} - CH_2]^+$: m/z 770 ($n = 5$) and 869 ($n = 6$).

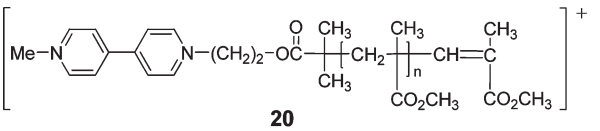

20

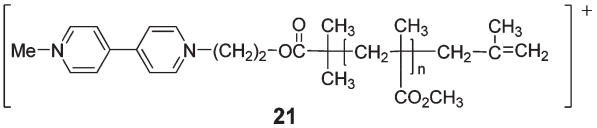

21

MALDI-TOF results for the crown-terminated polystyrene sample **15** in dithranol and AgTFA show the existence of the end groups (Figure 4). The main series of peaks at m/z 2708 ($n = 25$), 2812 ($n = 26$), and 2916 ($n = 27$) correspond to the silver adduct of polystyrene with no end groups (structure **22**). The loss of the MPPP32C10 moiety is believed to occur via a McLafferty-type rearrangement and cleavage one bond removed from the carbonyl group as shown in Scheme 7. The benzylidene end (the other terminal group) of the structure **22** arises from loss of hydrogen chloride. In the other series of peaks, the terminal crown ether unit (MPPP33C10) and chloride are both observed as silver adducts; Ag^+ is believed to be captured by the MPPP32C10 moiety (**15** + Ag^+): m/z 2726 ($n = 19$) and 2830 ($n = 20$).

MALDI-TOF mass spectrometric results for the crown-centered polystyrene sample **17** in 3-anthraquinoline are shown in Figure 5. Only one series is observed, and the sequential pairs of peaks are separated by 104 mass units, corresponding to the stryryl repeat unit. The BMP32C10 crown ether unit and two chloride end groups are observed in

Scheme 5. Proposed Mechanism for Generation of the Structure 20 Series from the Cleavage of the PMMA Main Chain by a Rearrangement

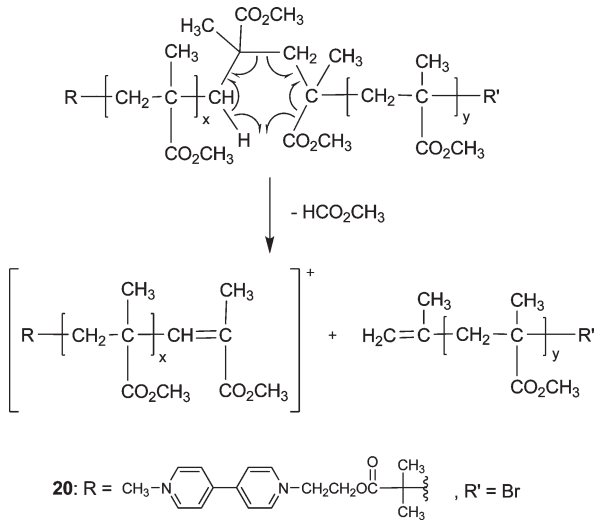

Scheme 6. Proposed Mechanism for Generation of the Structure 21 Series from the Cleavage of the PMMA Main Chain by a Rearrangement

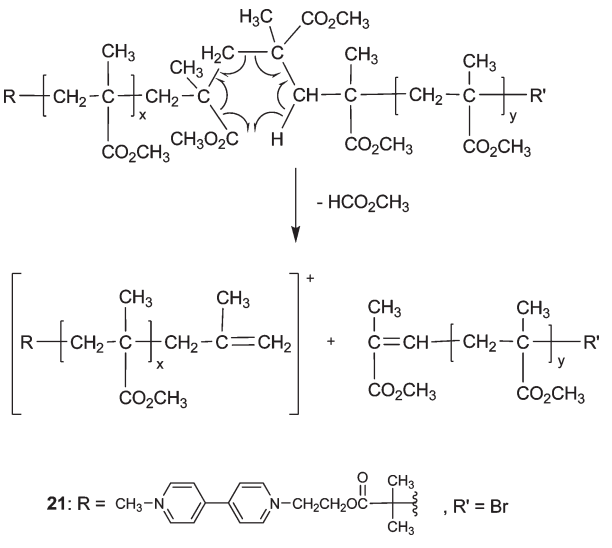

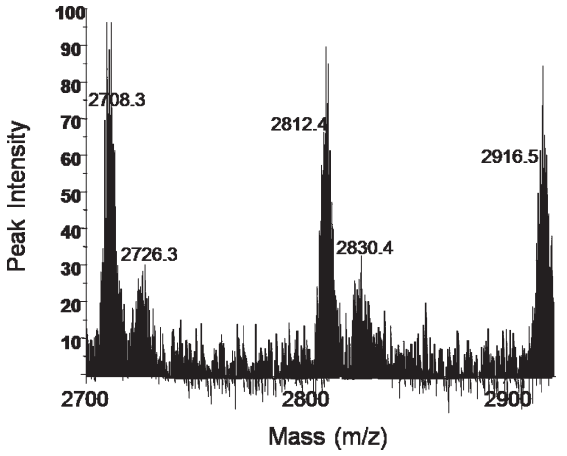

Figure 4. Partial MALDI-TOF mass spectrum (covering mass range 2700−2930 Da) of MPPP33C10-terminated polystyrene **15**. Sample prepared by the D-D method in dithranol with AgTFA as a cationization agent.

the spectrum; the charge results from inclusion of potassium ions presumably captured by the crown ether rings (**23**): m/z 4014 ($n+m=31$), 4118 ($n+m=32$), and 4222 ($n+m=33$). Even though the ATRP was catalyzed by copper(I) bromide, no bromide end or unsaturated terminal moiety is observed. From these results, we conclude that the chloride from the initiator was not exchanged to bromide during the ATRP, even though a different copper(I) halide (CuBr) was used as the catalyst.

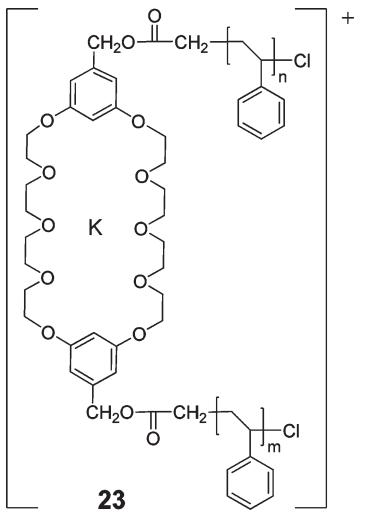

In MALDI-TOF mass analysis of the paraquat-terminated polymers, the paraquat moiety is clearly observed after loss of two PF_6 species. Whereas the TEMPO and the bromide end groups were not detected, the structures with unsaturated ends after loss of TEMPO and bromide were observed. Interestingly, for the polymers from ATRP with chloride initiators, the terminal chloride is clearly shown in the mass spectra, and no unsaturated end is observed when no cationization agent was used.

Formation of [2]Pseudorotaxanes from Polymers and Small Molecules (1 and 2 in Figure 1). The binding of the host- and guest-functionalized polymers with small molecules leads to the pseudorotaxanes **1** and **2**. The complexation between host and guest molecules was visually confirmed by a color change; the yellow or yellow-orange color is due to a charge transfer interaction between the electron-poor paraquat and the electron-rich phenyl rings of the crown ethers.[14] In panel **a** of Figure 6, the chloroform solution of the paraquat-terminated polystyrene **11** was colorless, but the solution turned yellow after addition of dibenzo-30-crown-10 (DB30C10) (right vial) or DB30C10-based cryptand[15] (center vial). In panel **b** of Figure 6, the chloroform solution of the crown ether (BMP32C10)-centered polystyrene **17** was colorless (left vial). However, the color changed to yellow after addition of paraquat diol (*N,N′*-bis(2-hydroxyethyl)-4,4′-bipyridinium $2PF_6^-$, center vial) or the paraquat-terminated polystyrene **11** (right vial). These color changes show that (1) the terminal pseudorotaxane polymers **1** were formed (panel **a**), (2) central pseudorotaxane polymer **2** was formed (panel **b**), and (3) the right vial in (panel b) contains a three-armed star polymer (**4**).

Isothermal macrocalorimetric (ITC) titration can be used to quantify host−guest binding. The association constants between the paraquat-terminated polystyrene **11** and BMP-32C10 and between the paraquat-terminated PMMA **13** and

Scheme 7. Proposed Mechanism for Generation of the Structure 22 Series by a McLafferty-Type Rearrangement

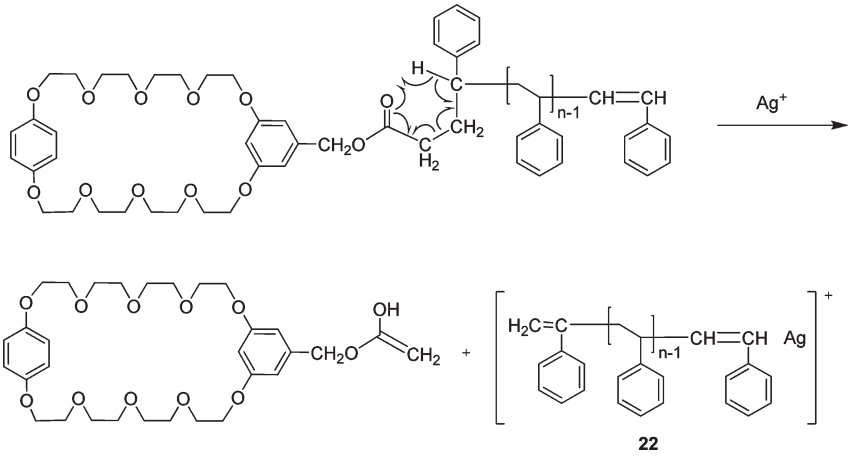

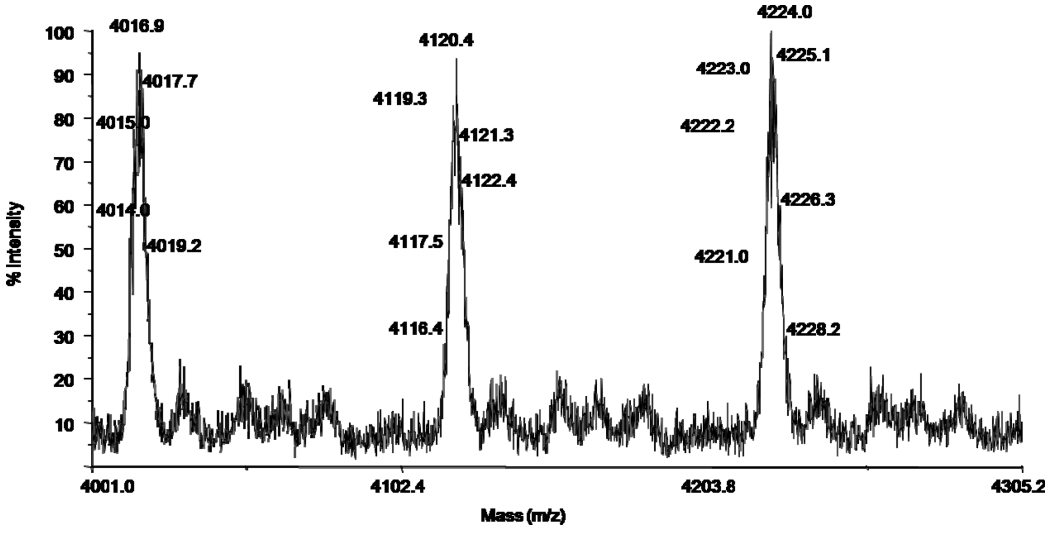

Figure 5. Partial MALDI-TOF mass spectrum (covering mass range 4001−4305 Da) of BMP32C10-centered polystyrene **17**. Sample prepared by the D-D method in 3AQ and no added cationization agent.

BMP32C10 were measured in chloroform at 25 °C: K_a = $(2.97 \pm 0.09) \times 10^3$ M^{-1} and $K_a = (3.63 \pm 0.10) \times 10^2$ M^{-1}, respectively. The association constants of paraquat and crown ether compounds in chloroform were measured for the first time; they were 4−6-fold higher than that of the small molecular host and guest analogues.[4a] As mentioned in the Introduction, the main intermolecular forces for complexations of crown ethers and paraquat derivatives are multiple hydrogen bonds, dipole−dipole, and π-electron interactions. Because of the lower polarity of chloroform relative to acetone, the interactions are stronger than in the higher polarity acetone medium. The stronger interactions gave higher K_a values in chloroform. Surprisingly, however, the binding of the paraquat PMMA **13** with BMP32C10 was almost 9-fold lower than that of the paraquat polystyrene **11** with BMP32C10. This decrease could be due to the interactions of the ester moieties of PMMA with the paraquat species. Perhaps one of the major interactions is hydrogen bonding between ester oxygen atoms and the aromatic protons of the paraquat units in the relatively nonpolar chloroform solution. This hypothesis is supported by the observation that the chemical shifts of the pyridinium protons of paraquat-terminated PMMA in $CDCl_3$ are very similar to those of dimethyl paraquat in acetone-d_6, as noted above.

Polymer−Polymer Binding (3, 4, 5, and 6 in Figure 1). The polymer−polymer binding of the functionalized polymers was also investigated. Chain extension by self-assembly (**3** in Figure 1) was observed by color and viscosity changes. The individual chloroform solutions of the paraquat-terminated polystyrene **11** and the crown ether-terminated polystyrene **15** were colorless. However, when the two polymers were dissolved in a 1:1 molar ratio in chloroform, the solution became yellow as with the other complexation systems in Figure 6. Viscometry provided evidence of chain extension by self-assembly in the solution (Figure 7). The intrinsic viscosity of the paraquat-terminated polystyrene **11** was 0.270 dL/g, and that of the crown ether-terminated polystyrene **15** was 0.171 dL/g in chloroform. However, the intrinsic viscosity of a 1:1 molar ratio solution of the two polymers was 0.321 dL/g. This clearly demonstrates that the two polymers interact and bind to form a chain-extended larger supramolecule (**3**).

A three-armed star polymer was formed from crown ether (BMP32C10)-centered polystyrene **17** and the paraquat-terminated polystyrene **11** in chloroform, as shown by the yellow color in panel b of Figure 6.Viscosity change also supports the formation of a star polymer formation in solution (Figure 8). The intrinsic viscosity of a 1:1 molar ratio solution of the two polymers was 0.389 dL/g in chloroform;

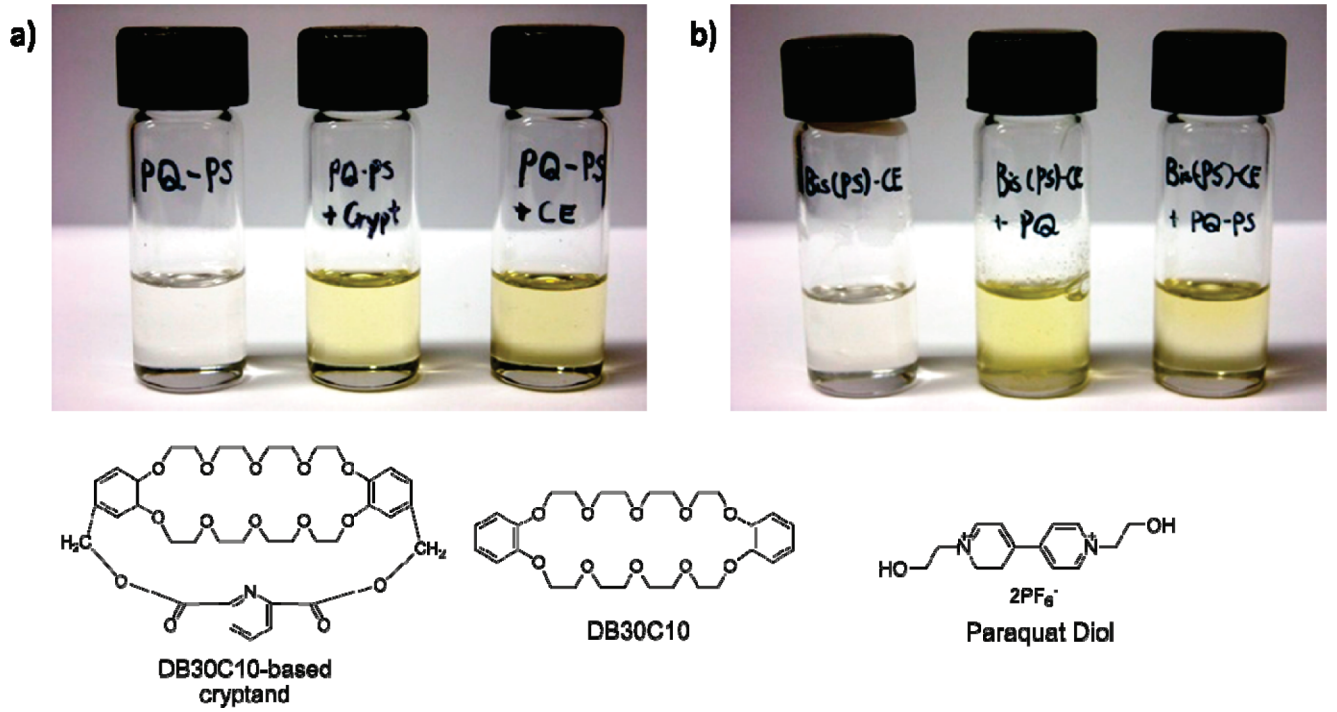

Figure 6. Qualitative visual test of complexation: (a) chloroform solutions of, from the left: paraquat-terminated polystyrene **11**, paraquat-terminated polystyrene **11** + DB30C10-based cryptand **11**, paraquat-terminated polystyrene **11** + BMP32C10. (b) From the left: crown ether-centered polystyrene **17** in chloroform, crown ether-centered polystyrene **17** + paraquat diol in acetone/$CHCl_3$ 1/1, and crown ether-centered polystyrene **17** + paraquat-terminated polystyrene **11** in $CHCl_3$.

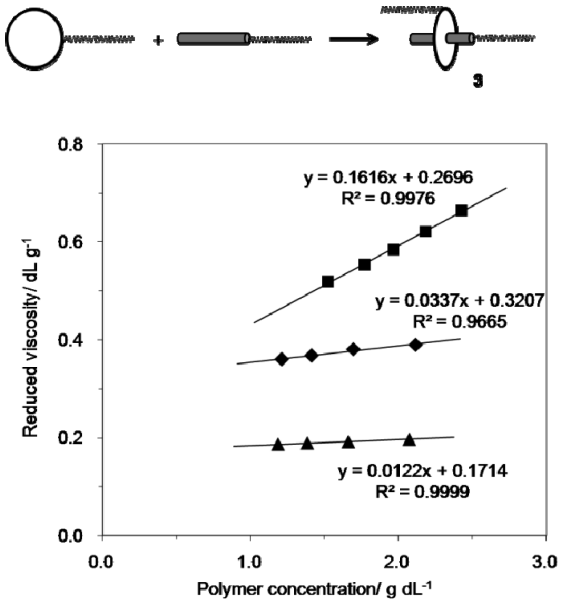

Figure 7. Reduced viscosity of paraquat-terminated polystyrene **11** (squares), MPPP32C10-centered polystyrene **15** (triangles), and 1:1 (molar ratio) solutions of the two polymers (diamonds), in $CHCl_3$ at 25 °C.

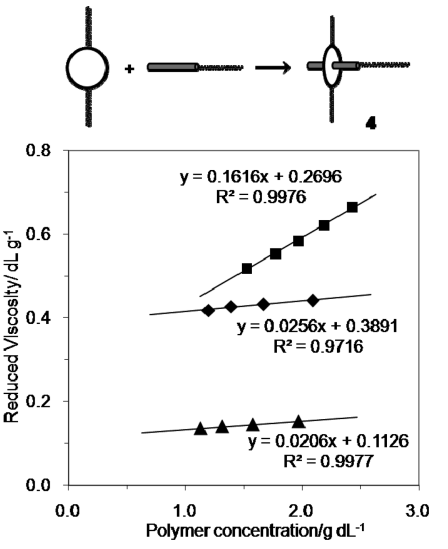

Figure 8. Reduced viscosity of paraquat-terminated polystyrene **11** (squares), BMP32C10-centered polystyrene **17** (triangles), and a 1:1 (molar ratio) solution of the two polymers (diamonds), in $CHCl_3$ at 25 °C.

the intrinsic viscosities of the paraquat-terminated polystyrene **11** and the crown ether-centered polystyrene **17** were 0.270 and 0.113 dL/g, respectively. The polymer−polymer binding to form the three-armed star polymer **4** in the solution leads to an increased hydrodynamic volume and hence the viscosity increase.

The expected complexation of the two polymers to form a star polymer was confirmed by NMR spectroscopy (Figure 9). The chemical shift changes of the crown ether protons of **17** in the ^1H NMR spectrum are clear evidence of the formation of the three-armed star polymer (**4**). The ethyleneoxy protons of the uncomplexed **17** appear at δ 3.97, 3.77, and 3.64 (bottom spectrum). However, they shifted to δ 3.88 and 3.73, and the upfield peak was resolved into peaks at δ 3.67 and 3.65 (upper spectrum) after adding 1 equiv of the paraquat polystyrene **11**. NMR does not easily afford a quantitative estimate of the association constant between two polymer species because the maximum chemical shift change (Δ_0) required to analyze this fast-exchange system is difficult to measure with polymeric substrates.[16]

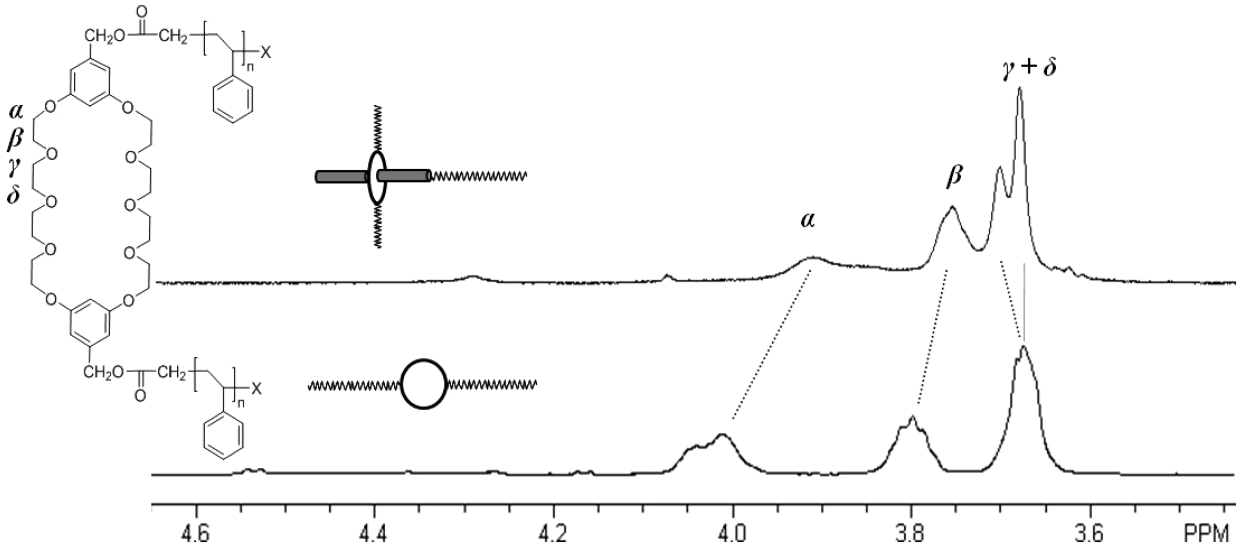

Figure 9. Partial 400 MHz ^{1}H NMR spectra of functional polystyrenes ($CDCl_3$, 23 °C). The bottom spectrum is BMP32C10-centered polystyrene **17** and the upper spectrum is the 1:1 (molar) mixture of BMP32C10-centered polystyrene **17** and PQ-terminated polystyrene **11**.

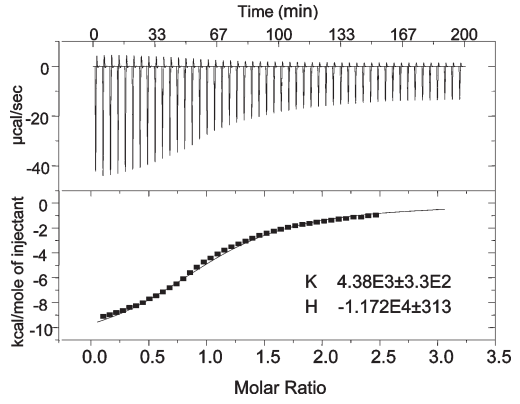

Figure 10. ITC titration curve (top: raw data; bottom: integrated heat flow and curve fit) and calculated physical constants of complexation between **11** (1.03 mM) and **17** (15.0 mM) in $CHCl_3$ at 25 °C. *K* is the association constant in M^{-1} units, and *H* is the enthalpy change in cal/mol.

Nonetheless, the NMR spectroscopic results confirm that the two polymeric species are bound to each other in solution. The fast-exchange process is analogous to that observed in the binding between the small molecules BMP32C10 and dimethylparaquat.[17]

However, ITC titration does afford an estimate of the association constant of this complexation (Figure 10). Into a chloroform solution of the paraquat polystyrene **11**, the crown ether polystyrene **17** solution was titrated and the heat flow was measured. The analysis indicates that K_a is $(4.38 \pm 0.33) \times 10^3$ M^{-1} ($CHCl_3$, 25 °C), and 1:1 stoichiometry was observed.

Copolymer formation from the host polystyrenes **15** or **17** with the paraquat-terminated PMMA **13** was investigated in the same manner. For diblock copolymer formation (**5**), the reduced viscosity plots of the individual polymers (**13** and **15**) and their 1:1 molar mixture are shown in Figure 11. The viscosity change was not very significant after mixing the two polymers due to weak binding between the paraquat unit of the PMMA and the crown ether unit of the polystyrene (**13**:[η] = 0.321 dL/g; **15**: [η] = 0.171 dL/g; **13** + **15**:[η] = 0.330 dL/g). The PMMA chain seems to interfere with the interaction of the paraquat and the crown ether moieties, as noted above with **13** and BMP32C10. In the same manner as

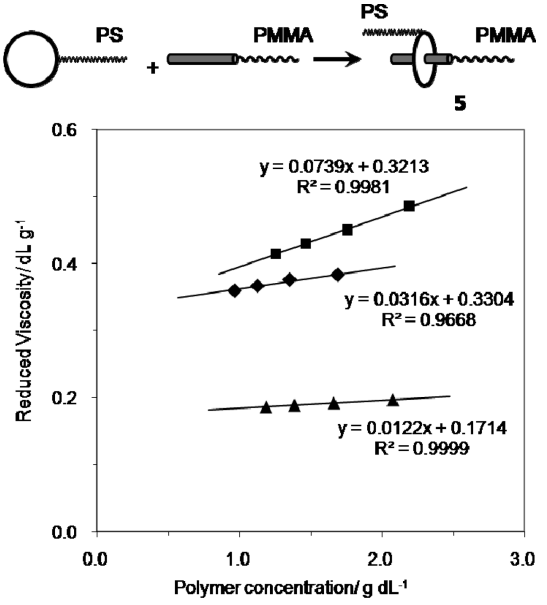

Figure 11. Reduced viscosity of paraquat-terminated PMMA **13** (squares), MPPP33C10-terminated polystyrene **15** (triangles), and 1:1 (molar ratio) solution of the two polymers (diamonds), in $CHCl_3$ at 25 °C.

the binding of **13** and BMP32C10 and as noted above, hydrogen bonding may occur between the ester oxygen atoms of PMMA and the paraquat units in the chloroform solution.

For three-armed copolymer formation (**6**), the reduced viscosity plots of the individual polymers (**13** and **17**) and their 1:1 mixture are shown in Figure 12. The viscosity change was not very significant for the same reason as the previous incomplete copolymer formation (**13**:[η] = 0.321 dL/g; **17**: [η] = 0.113 dL/g; **13** + **17**:[η] = 0.348 dL/g). When a solution of the two polymers (**13** and **17**) was cast on a glass plate, a turbid yellow film was formed. Macrophase separation was observed by optical microscopy.

Conclusions

Paraquat-terminated polystyrenes, paraquat-terminated poly(methyl methacrylate), and crown ether-centered or -terminated polystyrenes were synthesized by SFRP or ATRP. From these

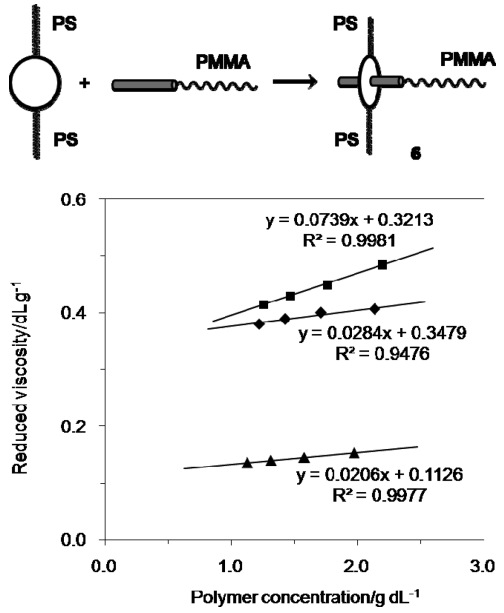

Figure 12. Reduced viscosity of paraquat-terminated PMMA **13** (squares), BMP32C10-centered polystyrene **17** (triangles), and 1:1 (molar ratio) solution of the two polymers (diamonds), in $CHCl_3$ at 25 °C.

polymers, pseudorotaxane polymers (**1** and **2**), chain extended (**3**), and three-armed star polymers (**4**) were formed by self-assembly in solution. The association constants for interaction of BMP32C10 and a DB30C10-based cryptand with the paraquat-terminated polystyrene were measured in chloroform for the first time. The K_a values were 4−6-fold higher than that measured for the binding of the corresponding small molecular hosts and guest in acetone-d_6. The linear and three-armed polystyrene−PMMA copolymers (**5** and **6**) were also formed in the same way; however, the PMMA paraquat system displays lower association constants. More powerfully binding systems, such as cryptand−guest or other multivalent host−guest, with higher association constants will be required to form self-assembled polystyrene−PMMA block copolymers that have properties similar to conventional covalently bound copolymers. Overall, the present results demonstrate that pseudorotaxane formation provides a unique method for reversible formation of chain extended, star and block polymers. We plan to utilize our new host systems[15] for these purposes in our future efforts.

Acknowledgment. We acknowledge financial support of this research by the National Science Foundation through DMR 0704076. We thank Dr. Tim Long and his group (VPI&SU) for performing the SEC analyses.

Supporting Information Available: ^{1}H NMR spectra of synthesized initiators and polymers and ITC titration graphs for complexation studies. This material is available free of charge via the Internet at http://pubs.acs.org.

References and Notes

(1) Pedersen, C. *J. Am. Chem. Soc.* **1967**, *89*, 7017–7036.
(2) An, H.; Bradshaw, J. S.; Izatt, R. M. *Chem. Rev.* **1992**, *92*, 543–572. An, H.; Bradshaw, J. S.; Izatt, R. M.; Yan, Z. *Chem. Rev.* **1994**, *94*, 939–991. Izatt, R. M.; Pawlak, K.; Bradshaw, J. S. *Chem. Rev.* **1995**, *95*, 2529–2586. Arnaud-Neu, F.; Delado, R.; Chaves, S. *Pure Appl. Chem.* **2003**, *75*, 71–102. Gokel, G. W.; Leevy, W. M.; Weber, M. E. *Chem. Rev.* **2004**, *104*, 2723–2750. Braunschweig, A. D.; Ronconi, C. M.; Han, J.-Y.; Cantrill, S. J.; Stoddart, J. F.; Khan, S. I.; White, A. J. P.; Williams, D. J. *Eur. J. Org. Chem.* **2006**, *2006*, 1857–1866. Han, T.; Chen, C.-F. *J. Org. Chem.* **2007**, *72*, 7287–7293.
(3) For reviews of pseudorotaxanes and rotaxanes see: Gibson, H. W.; Marand, H. *Adv. Mater.* **1993**, *5*, 11–21. Gibson, H. W.; Bheda, M. C.; Engen, P. T. *Prog. Polym. Sci.* **1994**, 843–945. Amabilino, D. B.; Stoddart, J. F. *Chem. Rev.* **1995**, *95*, 2725–2828.Gibson, H. W. In *Large Ring Molecules*; Semlyen, J. A., Ed.; John Wiley & Sons: New York, 1996; pp 191−262. Sauvage, J. P.; Dietrich-Buchecker, C. O. *Molecular Catenanes, Rotaxanes and Knots*; Wiley-VCH: Weinheim, 1999.Raymo, F. M.; Stoddart, J. F. *Chem. Rev.* **1999**, *99*, 1643–1664. Hublin, T. J.; Busch, D. H. *Coord. Chem. Rev.* **2000**, *200*−202, 5–52. Takata, T.; Kihara, N. *Rev. Heteroat. Chem.* **2000**, *22*, 197–218. Mahan, E.; Gibson, H. W. In *Cyclic Polymers*; Semlyen, J. A., Ed.; Kluwer Academic Publishers: Dordrecht, The Netherlands, 2000; pp 415−560.Collin, J.-P.; Heitz, V.; Sauvage, J.-P. *Top. Curr. Chem.* **2005**, *262*, 26–62. Huang, F.; Gibson, H. W. *Prog. Polym. Sci.* **2005**, *30*, 982–1018. Wenz, G.; Han, B.-H.; Muller, A. *Chem. Rev.* **2006**, *106*, 782–817. Vickers, M. S.; Beer, P. D. *Chem. Soc. Rev.* **2007**, *36*, 211–225. Tian, H.; Wang, Q.-C. *Chem. Soc. Rev.* **2006**, *35*, 361–374. Griffiths, K.; Stoddart, J. F. *Pure Appl. Chem* **2008**, *80*, 485–506. Suzaki, Y.; Taira, T.; Osakada, K.; Horie, M. *Dalton Trans.* **2008**, 4823–4833. Ogoshi, T.; Harada, A. *Sensors* **2008**, *8*, 4961–4982. Crowley, J. D.; Goldup, S. M.; Lee, A.-L.; Leigh, D. A.; McBurney, R. T. *Chem. Soc. Rev.* **2009**, *38*, 1530–1541. Harada, A.; Takashima, Y.; Yamaguchi, H. *Chem. Soc. Rev.* **2009**, *38*, 875–882. Wenz, G.; Yui, N.; Katoono, R.; Yamashita, A.; Li, J.; Tonelli, A. E. *Adv. Polym. Sci.* **2009**, *222*, 1–54.
(4) (a) Allwood, B. L.; Shahriari-Zavareh, H.; Stoddart, J. F.; Williams, D. J. *J. Chem. Soc., Chem. Commun.* **1987**, 1058–1061. Allwood, B. L.; Spencer, N.; Shahriari-Zavareh, H.; Stoddart, J. F.; Williams, D. J. *J. Chem. Soc., Chem. Commun.* **1987**, 1061–1064. Allwood, B. L.; Spencer, N.; Shahriari-Zavareh, H.; Stoddart, J. F.; Williams, D. J. *J. Chem. Soc., Chem. Commun.* **1987**, 1064–1066. Ashton, P. R.; Slawin, A. M. Z.; Spencer, N.; Stoddart, J. F.; Williams, D. J. *J. Chem. Soc., Chem. Commun.* **1987**, 1066–1069. (b) Delaviz, Y.; Merola, J. S.; Berg, M. A. G.; Gibson, H. W. *J. Org. Chem.* **1995**, *60*, 516–522. Asakawa, M.; Ashton, P. R.; Boyd, S. E.; Brown, C. L.; Gillard, R. E.; Kocian, O.; Raymo, F. M.; Stoddart, J. F.; Tolley, M. S. *J. Org. Chem.* **1997**, *62*, 26–37. Bryant, W. S.; Guzei, L. A.; Rheingold, A. L.; Merola, J. S.; Gibson, H. W. *J. Org. Chem.* **1998**, *63*, 7634–7639. Bryant, W. S.; Guzei, I. A.; Rheingold, A. L.; Gibson, H. W. *Org. Lett.* **1999**, *1*, 47–50. Jones, J. W.; Zakharov, L. N.; Rheingold, A. L.; Gibson, H. W. *J. Am. Chem. Soc.* **2002**, *124*, 13378–13379.
(5) Gibson, H. W.; Yamaguchi, N.; Hamilton, L. M.; Jones, J. W. *J. Am. Chem. Soc.* **2002**, *124*, 4653–4665.
(6) Huang, F.; Gibson, H. W. *J. Am. Chem. Soc.* **2004**, *126*, 14738–14739.
(7) Jones, J. W.; Bryant, W. S.; Bosman, A. W.; Janssen, R. A. J.; Meijer, E. W.; Gibson, H. W. *J. Org. Chem.* **2003**, *68*, 2385–2389. Newkome, G. R.; Kim, H. J.; Choi, K. H.; Moorefield, C. N. *Macromolecules* **2004**, *37*, 6268–6274. Beil, J. B.; Zimmerman, S. C. *Chem. Commun.* **2004**, 488–489. Pittelkow, M.; Christensen, J. B.; Meijer, E. W. *J. Polym. Sci., Part A: Polym. Chem.* **2004**, *42*, 3792–3799.
(8) Huang, F.; Nagvekar, D. S.; Slebodnick, C.; Gibson, H. W. *J. Am. Chem. Soc.* **2005**, *127*, 484–485.
(9) Gibson, H. W.; Ge, Z.; Huang, F.; Jones, J. W.; Lefebvre, H.; Vergne, M. J.; Hercules, D. M. *Macromolecules* **2005**, *38*, 2626–2637.
(10) Tundo, P.; Kippenberger, D.; Politi, M. J.; Klahn, P.; Fendler, J. H. *J. Am. Chem. Soc.* **1982**, *104*, 5352–5358.
(11) Gibson, H. W.; Nagvekar, D. S. *Can. J. Chem.* **1997**, *75*, 1375–1384.
(12) Dourges, M.-A.; Charleux, B.; Vairon, J.-P.; Blais, J.-C.; Bolbach, G.; Tabet, J.-C. *Macromolecules* **1999**, *32*, 2495–2502.
(13) Jackson, A. T.; Yates, H. T.; Scrivens, J. H.; Green, M. R.; Bateman, R. H. *J. Am. Soc. Mass Spectrom.* **1997**, *8*, 1206–1213.
(14) Huang, F.; Gibson, H. W.; Bryant, W. S.; Nagvekar, D. S.; Fronczek, F. R. *J. Am. Chem. Soc.* **2003**, *125*, 9367–9371.
(15) (a) Pederson, A. M.-P.; Vetor, R. C.; Rouser, M. A.; Huang, F.; Slebodnick, C.; Schoonover, D. V.; Gibson, H. W. *J. Org. Chem.* **2008**, *73*, 5570–5573. (b) Pederson, A. M. P.; Ward, E. M.; Schoonover, D. V.; Slebodnick, C.; Gibson, H. W. *J. Org. Chem.* **2008**, *73*, 9094–9101.
(16) For fast exchange host−guest systems in proton NMR, only time-averaged peaks appear, as with our current system. In this case, the maximum chemical shift change (Δ_0) is required to calculate K_a by NMR. Usually Δ_0 can be measured by keeping the concentration of one component constant and increasing that of the other to very high values;

then a plot of the chemical shift versus the inverse of the concentration of the variable component yields Δ_0 as the zero intercept. See: Tsukube, H.; Furita, H.; Odani, A.; Takeda, Y.; Kudo, Y.; Inoue, Y.; Liu, Y.; Sakamoto, H.; Kimura, K. In *Comprehensive Supramolecular Chemistry*; Atwood, J. L., Davies, J. E. D., MacNicol, D. D., Vögtle, F., Exec. Eds.; Pergamon: New York, Vol. *8*, Chapter 10, pp 425−482. However, in our systems in which both host and guest are polymeric, but contain only a single active site, there is a practical limit to how high the concentration can be before high viscosity broadens the peak too much to accurately measure the chemical shift change.

(17) Zhang, J.; Zhai, C.; Wang, F.; Zhang, C.; Li, S.; Zhang, M.; Li, N.; Huang, F. *Tetrahedron Lett*. **2008**, 5009–5012.